PERGAMON

Planetary and Space Science 49 (2001) 1643–1653

Planetary and Space Science

www.elsevier.com/locate/planspasci

Particle populations in Mercury's magnetosphere

Peter Wurz[a,*], Lars Blomberg[b]

[a] *Physics Institute, University of Bern, Sidlerstrasse 5, CH-3012 Bern, Switzerland*
[b] *Royal Institute of Technology, Kungl Tekniska Högskolan, SE-100 44 Stockholm, Sweden*

Abstract

Observations by Mariner 10 during its first and third flybys showed that Mercury possesses an intrinsic magnetic field resulting in a small magnetosphere that can keep the solar wind from directly interacting with the planet's surface under usual conditions. Since Mercury occupies a large fraction of its magnetosphere, regions of trapped charged particles in the inner magnetosphere, the plasmasphere and the energetic radiation belts, would all be absent. During the first flyby, energetic particle bursts were detected and interpreted as hermean substroms analogous to the terrestrial magnetosphere. Moreover, during this flyby, ULF waves and field-aligned currents were detected in the data. Earth-based observations of Na, K, and Ca populations in the exosphere strongly suggest the existence of dynamic magnetospheric processes at high latitudes interacting with the planet's surface.

1. Introduction

Observations by Mariner 10 during its first and third flybys showed that Mercury possesses an intrinsic magnetic field (Ness et al., 1974b; Connerney and Ness, 1988) resulting in a magnetosphere, compatible with the estimated planetary magnetic field and solar wind pressure (Ogilvie et al., 1974; Ness et al., 1976). The possibility that Mercury would be found to possess a significant global magnetic field and magnetosphere was thought to be extremely remote before the Mariner 10 Mercury flyby (Ness, 1979). Bow shock and magnetopause crossings were detected at locations in approximate agreement with the calculated overall shape of the magnetosphere, although the first and the third flyby were on the planet's night side passing the planet closely. In addition, energetic particle bursts, interpreted as substorm-like features, were detected (Simpson et al., 1974b), as well as ULF waves (Russell, 1989) and field-aligned currents (Slavin et al., 1997). Earth-based observations of sodium and potassium populations in the exosphere strongly suggest the existence of dynamic magnetospheric processes at high latitudes (Potter and Morgan, 1985, 1986). Recently, exospheric calcium populations close to the poles have also been found (Bida et al., 2000).

The size of the hermean magnetosphere is only about 5% of that of the Earth, although the planetary radii differ by less than a factor three. When scaled to the planet size, the hermean magnetosphere is a factor of about seven smaller than the Earth's. The subsolar point of the magnetopause is located at about $1.1–1.5R_M$ from Mercury's centre (Ness et al., 1976; Ogilvie et al., 1977) with the planetary radius $R_M = 2440$ km. A more recent estimate for this location is $1.35 \pm 0.02R_M$ (Russell et al., 1988). This small stand-off distance of the magnetopause means that Mercury occupies a much larger relative volume inside its magnetosphere. Simply because of the size alone, regions of trapped charged particles in the inner magnetosphere, i.e., the plasmasphere and the energetic radiation belts, would all be absent. Moreover, the weak magnetic field results in ion gyro radii exceeding the distance to the subsolar point of the magnetopause already at modest ion energies. The difference between the scale of the two magnetospheres sizes alone leads to a significantly more dynamic hermean magnetosphere. Mercury's close proximity to the Sun even enhances this effect.

The absence of an ionosphere at Mercury poses a significant problem for the closure of the magnetospheric current system. The existence of high field-aligned currents requires a sufficiently conducting layer close to the surface of Mercury. The ionosphere at Earth provides a good conductor for the currents needed to sustain the shape and dynamics of the magnetosphere. There is considerable uncertainty as to how this current system, if it exists, closes at Mercury. Closure, albeit difficult, can either be established via the ionised component of the exosphere (Lundin et al., 1997) or via the planetary regolith. Also, a sheath of photoelectrons close

* Corresponding author. Tel.: +41-31-631-4426; fax: +41-31-631-4405.
E-mail address: peter.wurz@soho.unibe.ch (P. Wurz).

0032-0633/01/$ - see front matter
PII: S0032-0633(01)00102-7

to the sunlit surface may act as a conductor (Grard, 1997; Grard et al., 1999). However, none of these theories have been tested yet.

The solar wind strongly drives the magnetosphere of Mercury, since it has low inertia due to its small size and the lack of trapped charges, as well as the stronger solar wind at the location of Mercury than at Earth. For testing our understanding of magnetospheric dynamics, Mercury is of particular importance to the magnetospheric physics community because of the many similarities with the Earth's magnetosphere and on the other hand because of some key differences. The probable lack of a plasmasphere and ionosphere at Mercury provides an opportunity to determine the importance of the ionosphere in magnetospheric dynamics. Mercury could be more useful than Jupiter in that respect, since for Jupiter, centrifugal forces play a dominant role, and the dynamics are not directly comparable with those at Earth.

Since the initial publications of plasma electrons (Ogilvie et al., 1974), energetic particles (Simpson et al., 1974b), and the following detailed publications of these observations (Ogilvie et al., 1977; Eraker and Simpson, 1986), there have been a few more general reviews on this topic (e.g. Russell et al., 1988). In the absence of new observational data many recent publications report on theoretical aspects (Goldstein et al., 1981; Baker et al., 1986; Cheng et al., 1987) and lately more so on computer simulations of the hermean magnetosphere either based on Mariner 10 data or performed in a more general way (Ip, 1986, 1997; Luhmann et al., 1998; Kabin et al., 2000). A better understanding of the magnetospheric current systems is necessary for further progress and requires more information about the conductivities of the surface and exosphere. A major uncertainty for all modelling work is the possibility that the solar wind may reach the planet's surface at least at times of fast changing pressure and/or interplanetary magnetic field configuration, which favours magnetic reconnection in the dayside magnetosphere. Goldstein et al. (1981) have estimated that the solar wind may reach the planet's surface for only 6% of the time. However, if the solar wind is actually able to compress the dayside magnetosphere such that it directly impacts the surface remains a topic of considerable controversy (cf., Slavin et al., 1997; Kabin et al., 2000). If solar wind reaches the surface at least occasionally, the magnetospheric current systems would have topologies significantly different from those observed at Earth. For example, coronal mass ejections with strong southward oriented interplanetary magnetic field have the potential to almost completely expose the planet's surface to the solar wind (Luhmann et al., 1998).

2. Instrumentation of Mariner 10

Mariner 10 was a three-axis stabilised spacecraft, which carried three instruments that contributed to the discovery and the understanding of the magnetosphere: two tri-axial fluxgate magnetometers (Ness et al., 1974a, b), a plasma science instrument (Ogilvie et al., 1977), and an energetic particle detector (Simpson et al., 1974a). We will describe the latter two instruments in some detail since data recorded with these instruments will be covered in this review.

The plasma science instrument consisted of a rather sophisticated ion and electron sensor observing in the sunward direction and a less elaborate electron analyser observing in the anti-sunward direction (Ogilvie et al., 1977). These sensors were mounted on a motor-driven scan platform which could operate at a scan rate of either one or four degrees per second, with the former rate being used at Mercury and the scan axis within a few degrees of the normal to the ecliptic plane. As a result of an unexplained problem immediately after launch, the sunward-facing sensor did not operate properly and never detected counts above the cosmic ray background. Hence, all conclusions about the nature of the low-energy plasma environment of Mercury come from the rear-facing sensor. This sensor was a hemispherical electrostatic analyser accepting electrons in the energy range from 13 to 688 eV. The energy range was divided into 15 logarithmically spaced energy channels of $\Delta E/E = 0.066$ width. The detector was stepped continuously through these 15 energy steps dwelling at each step for 0.4 s, and a total spectrum was obtained after 6 s. Outside the hermean magnetosphere the sensor measured typical interplanetary solar wind electron spectra (Ogilvie et al., 1974), which we will not discuss here. An important and complicating aspect of the quantitative analysis of data from this sensor was the significant and varying electrical potential of the Mariner 10 spacecraft (Ogilvie et al., 1977).

The energetic particle detector consisted of two telescopes, the main telescope (MT) and the low energy telescope (LET) (Simpson et al., 1974a; Eraker and Simpson, 1986). These energetic particle telescopes provided measurements of the energy loss, total energy, and range of particles that entered the telescope. The two telescopes performed successfully during the Mercury encounters and provided significant observations of transient events. The MT consisted of six detectors inside a plastic scintillator that was in anti-coincidence with the telescope elements. The energy losses in three of the detectors (1, 2, and 5) were determined by 256-channel pulse-height analysers. The low-energy counting rate of the MT responded to protons and helium in the energy range 0.62–10.3 MeV/nucleon (ID1 accumulator) and the energy range extended up to 68 MeV/nucleon. The MT responded to electrons with energies from 170 keV (efficiency of 0.08) up to 30 MeV with a peak efficiency of 0.70 at 840 keV. The LET was designed to measure low-energy protons and helium nuclei in the presence of a high intensity of low-energy electrons. The LET was designed to measure protons in two energy ranges 0.53–1.9 and 1.9–8.9 MeV. Electrons with energies of up to approximately 600 keV were detected during portions of these electron bursts. Ambiguities in the interpretation of the data recorded with this instrument

Table 1
The capabilities of the particle and fields instrumentation used during the Mariner 10 flybys

Instrument	Range	Comments	Reference
Fluxgate magnetometer	± 16 nT, ± 128 nT	Up to ± 3188 nT bias field	Ness et al. (1974a, b)
Electron analyser	13.4–688 eV	13 logarithmically spaced channels	Ogilvie et al. (1977)
Energetic particle detector, MT	e^-: 170 keV–30 MeV p, α: 0.62–68 MeV/nucleon	Range > 35 keV for e^- in case of pulse pile-up	Simpson et al. (1974a); Christon et al. (1979)
Energetic particle detector, LET	e^-: 170 keV–30 MeV p : 0.53–8.9 MeV	Range > 35 keV for e^- in case of pulse pile-up	Simpson et al. (1974a); Christon et al. (1979)

were pointed out by Armstrong et al. (1975, 1979). In a following calibration of a spare instrument, it was found that both telescopes had some sensitivity to low-energy electrons of energy greater than 35 keV due to pulse pile-up in the detectors (Christon et al., 1979; Eraker and Simpson, 1986).

In summary (see also Table 1), the particle instrumentation on Mariner 10 covered the energy range from 13 to 688 eV for plasma electrons, from 170 keV (> 35 keV in case of pulse pile-up) to 30 MeV for energetic electrons, and from 0.62 to 68 MeV for protons. Note that there is a substantial gap in the energy range from 688 eV to 170 keV that is not covered by instrumentation on Mariner 10, which prevented to establish the power spectrum of electrons in the energy range below 170 keV and hampered the scientific interpretation of the measured energetic particle data quite a bit.

3. Observations

The Mariner 10 spacecraft is the only spacecraft to have visited Mercury so far. Mariner 10 was launched on 2 November 1973 and encountered Mercury for the first time on 29 March 1974. Mariner 10 reencountered Mercury two more times, on 21 September 1974 and on 16 March 1975. Since the final orbit of Mariner 10 about the Sun was exactly twice the orbital period of the planet Mercury, all flybys occurred in an almost identical position with respect to the Sun when Mercury was at aphelion. During the first (M I) and the third encounter (M III) the spacecraft passed the planet at the night side, with the closest approach being 707 and 327 km, respectively. These two encounters entered Mercury's magnetosphere with the trajectories nearly parallel to Mercury's magnetic equator. Particle populations corresponding to magnetospheric plasma regions known from the magnetosphere of the Earth have been observed. The detailed trajectories of these two encounters have been given by Ness et al. (1975a). The second encounter (M II) was at the dayside of the planet with the closest approach being 50,000 km, far outside of Mercury's magnetosphere. An overview of the first encounter is shown in Fig. 1, where the spacecraft trajectory, the approximate locations of the bow shock and the magnetopause, the type of electron plasma, and high-energy particle data are given. Due to the high speed with which the spacecraft flew past the planet, the entire passage through the magnetosphere and magnetosheath from bow shock to bow shock required less than 35 min. In total, two such sets of magnetospheric data are available for Mercury. Comparison with the magnetosphere of the Earth indicates that these data sets consist primarily of near-tail and high-latitude polar cap observations (Russell et al., 1988; Slavin et al., 1997).

The complete particle and fields data for the first flyby are given in Fig. 2. For M I the inbound bow shock is clearly identified by the sharp rise in magnetic field magnitude, typical for a shock when the interplanetary magnetic field lies perpendicular to the bow shock normal (quasi-perpendicular shock) as is the case here. There are multiple crossings of the boundary as it moves back and forth at velocities greater than the spacecraft with the last crossing at 2028 UT. The diffuse nature of the outbound shock is caused by the interplanetary magnetic field being oriented almost parallel to the shock normal (quasi-parallel shock). Just inside the magnetopause cool magnetospheric electron plasma was found with characteristic energies of 20–70 eV and densities of $\sim 7\ \mathrm{cm}^{-3}$ (see Fig. 2, panels 6–8), distinct from interplanetary electron plasma or plasma in the magnetosheath (Ogilvie et al., 1974). No cold, dense plasmas indicative of ionospheric or plasmaspheric particles were observed even at closest approach, at 2046:38 UT. In this region, the magnetic field direction was generally anti-sunward and its magnitude increased steadily when approaching the planet. The magnetic field is consistent with a field produced by a planetary dipole, magnetopause current, and a neutral current sheet above the spacecraft (Ness et al., 1975b; Whang, 1977, 1979). Note that the direction of the interplanetary magnetic field was northward in the inbound magnetosheath and southward in the outbound magnetosheath. Hence, at some unknown time while the spacecraft was in Mercury's magnetosphere the interplanetary magnetic field switched from northward to southward orientation. At 2046:14 UT the electron plasma suddenly changed to a hotter spectrum with energies exceeding the energy range of the instrument, indicating the characteristic electron energies to be in the keV range or above (Ogilvie et al., 1977). From the magnetic field data it was deduced that the spacecraft crossed the cross-tail current sheet during this time.

Several major bursts of energetic particle flux enhancements were observed with the energetic particle detector

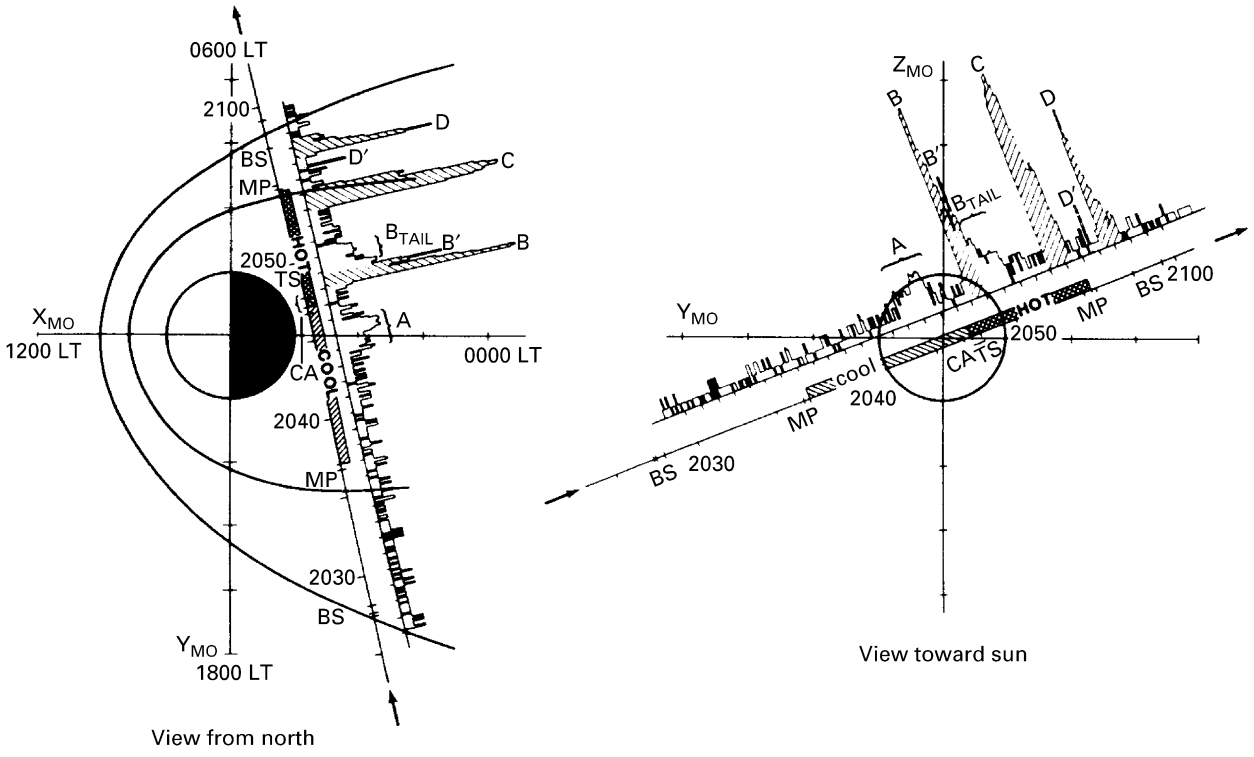

Fig. 1. The trajectory of Mariner 10 during the first encounter on day 88, 1974 (indicated by the arrows) is shown in Mercury orbital coordinates (X_{MO} is toward the sun, Y_{MO} is toward dusk, and Z_{MO} is toward the north celestial pole). The hatched and cross-hatched areas indicate cool and hot plasma regions, respectively. Offset from the trajectory curve is the ID1 counting rate (6 s resolution) in logarithmic representation. The shaded portion of the ID1 counting rate identifies electron fluxes with energies > 35 keV (due to pulse pile-up), otherwise energies are > 170 keV (figure from Christon, 1987).

and were labelled A, B, B′, C, D, and D′ (Simpson et al., 1974b). These data are shown in Fig. 2 in the uppermost panel. The particles were most likely electrons, and particle energies up to 600 keV were observed (Eraker and Simpson, 1986). Most of these energetic particle bursts show a complicated temporal structure with different rise-times, decays, peak intensities, and even pulsations during the events (Eraker and Simpson, 1986). These particle events and associated fields and plasma disturbances were interpreted to be most likely hermean substorms analogous to magnetospheric disturbances at Earth (Siscoe et al., 1975; Eraker and Simpson, 1986; Christon, 1987; and discussion below).

The third flyby seems to be most representative of a time when the Mercury magnetosphere was relatively stable. The complete plasma electron and magnetic field data for the third flyby are given in Fig. 3. The trajectory for M III was carefully designed to occur at higher latitude than M I and to have a closer miss distance to the planet in order to optimise the measurements of the intrinsic magnetic field of Mercury. There are no impulsive changes in the magnetic field inside the magnetosphere but only a gradual increase in magnitude as the spacecraft passes near the magnetic pole at closest approach. Note that the low-energy channels of the plasma electron sensor only recorded photoelectrons from the spacecraft, which presumably was at +90 V spacecraft potential, and therefore this data are not displayed in Fig. 3. On this trajectory, the inbound shock was the quasi-parallel shock and the outbound was the quasi-perpendicular shock. The M III passage was at higher latitudes and only cool plasma was observed inside the hermean magnetosphere, basically the "horns" of a cooler quiet-time plasma sheet (Ness et al., 1976; Ogilvie et al., 1977). Only a modest ionosphere was found at Mercury with an upper limit of the electron densities of 10^3 cm^{-3}. Near closest approach (CA was at 2239:23 UT) the spacecraft entered a region of very low electron intensities, presumably the extensions of the lobes of the magnetotail with open field lines connecting to the solar wind. Electron densities in this location were 0.1 cm^{-3} (Ogilvie et al., 1977). During the M III flyby the interplanetary magnetic field was pointing northward the whole time (Ness et al., 1976) so that dayside reconnection of the magnetic field is not as likely. In contrast to the first flyby, no large energetic particle event was detected during the third flyby (Eraker and Simpson, 1986). Also, field-aligned currents were not detected during this flyby (Slavin et al., 1997). Field-aligned currents and magnetospheric convection, in general, are known to decrease greatly in intensity during prolonged times of northward interplanetary magnetic field (Slavin et al., 1997). However, the total absence of field-aligned currents is somewhat surprising and perhaps this is a result of the orbital geometry.

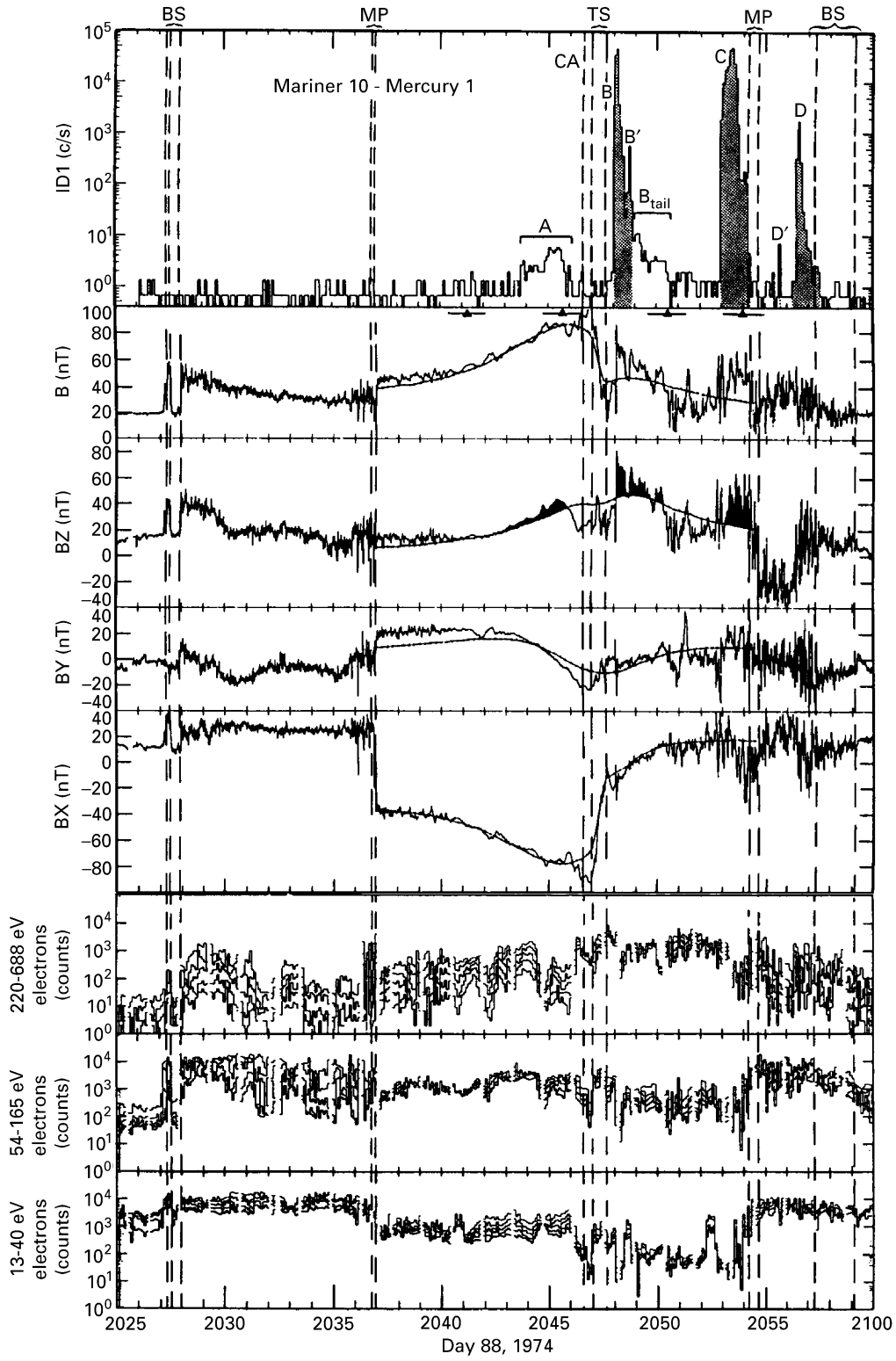

Fig. 2. Plot of energetic particle data, magnetic field data, and energetic electron data for M I. The magnetic field magnitude B and its components BZ, BY, and BX are given in Mercury orbital coordinates (0.2 s averages). The plasma electron data are given in three groups of five adjacent channels of the 15 logarithmically spaced channels from 13 to 688 eV. The dashed vertical lines indicate the bow shock (BS), the magnetopause (MP), the closest approach (CA), and the tail current sheet (TS). The magnetic field fit by Whang (1977, 1979) is shown as dotted curve. Deviations between the measured and calculated magnetic field are darkened in the plot and highlight possible dipolarisations. The shaded portion of the ID1 counting rate identifies electron fluxes with energies > 35 keV due to pulse pile-up, otherwise energies are > 170 keV (figure adapted from Christon, 1987).

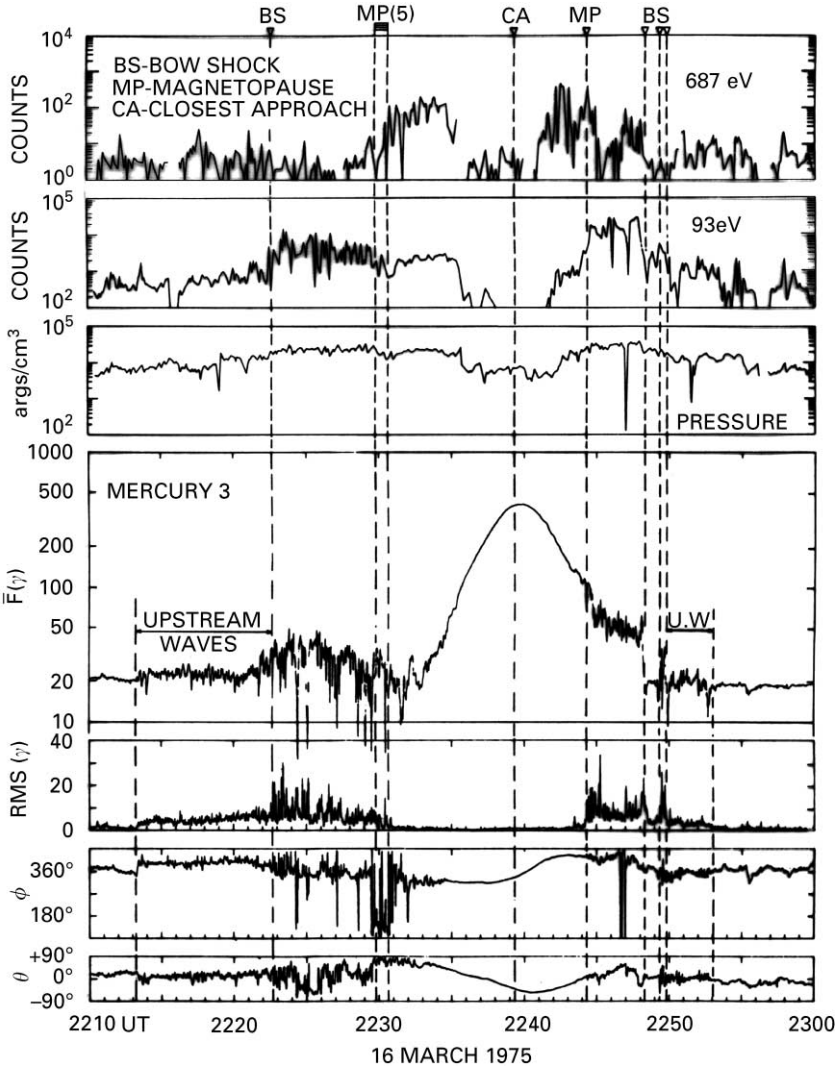

Fig. 3. Combined electron plasma and magnetic field observations for the M III flyby. Panels 1 and 2 respectively, show the electron plasma data for 688 and 93 eV, and panel 3 shows the pressure. The 13 eV channel is not shown because only photoelectrons from the spacecraft are measured at this energy during M III. Panels 4–7 show the magnitude, rms variation, azimuth and latitude angles of the magnetic field (figure adapted from Ogilvie et al., 1977).

4. Substorm phenomena

In analogy to the Earth's magnetosphere, the interaction of southward directed interplanetary magnetic field is favourable to the reconnection process in the hermean magnetosphere and leads to an increase in the energy stored in the magnetotail field (Siscoe et al., 1975). In addition, the tail field near the planet appears to be drawn out. A substorm is the phenomenon when this stored energy is dissipated, often in an explosive manner. As a consequence large amounts of energy can be injected into the exosphere. A typical signature of a substorm are the so-called dipolarisations in the magnetotail region in which the stretched-out magnetic field lines suddenly snap back to a dipolar-like configuration (e.g. McPherron et al., 1973; Ip, 1997, and references therein). Investigations at Mercury will give clues to the triggering of substorms, which is much more obscure in Earth's magnetosphere because of its very large inertia.

The major evidence for substorm-like phenomena at Mercury comes from the sudden entry into a region of hot electrons after closest approach during M I (Siscoe et al., 1975), and the observations of energetic particle bursts with the energetic particle detector (Simpson et al., 1974b). Moreover, the magnetic field appears to be strongly disturbed in this region, i.e., large deviations from the model field are observed (see Fig. 2), which is a further indication of substorm activity.

In the first flyby, the spacecraft entered the near-tail plasma sheet from below on the dusk side as can be seen in the right panel of Fig. 1, while the magnetosheath field was northward (see Fig. 2). The field just inside the magnetopause was tail-like and relatively quiet. Approaching the planet, the magnetic field increased with time. Shortly after

the closest approach, around 2047 UT, the magnitude decreased rapidly while the inclination increased to northward. This indicates a transition from tail-like field to dipole-like field orientation with a southward oriented planetary dipole. These large changes in magnetic field magnitude, the dipolarisations, occurred at the same time as the strong energetic particle bursts B, B′, and C were observed as can be seen in Fig. 2 (Christon, 1987). Even particle burst A is associated with a small magnetic field change. The energetic particles of event D are observed in the magnetosheath. Probably these particles are on draped sheath field lines lost through the magnetopause as the particle packet passes around the dayside of the planet (Russell et al., 1988).

By applying a simple scaled model of the Earth's magnetosphere to Mercury, Siscoe et al. (1975) showed that the time scales for substorms should be of the order of 1–2 min, commensurate with the duration of the energetic particle bursts. At high temporal resolution the energetic particle bursts reveal a lot of interesting structure. For example, Eraker and Simpson (1986) have pointed out that the B, B′, C, and D energetic particle bursts are highly modulated electron fluxes with periods of 5–10 s (pulsations). In a very detailed study of the B and B′ event, Christon (1987) identified four characteristic substorm time scales, the storage period, the release and recovery period, the multiple-onset period, and the pulsation period. From this study, it was found that substorm processes are on average a factor of 33 ± 11 shorter on Mercury than on Earth. This estimate compares favourably to the convection time scaling of 50 within a factor of two, i.e., $T_C \approx 1.2$ min at Mercury (Siscoe et al., 1975), which is the relevant time scale for the substorm process. However, one has to be cautious when applying scaled models since the planets do not scale in the same way as the magnetospheres and moreover the conductivity of the hermean ionosphere, planetary surface, or near-surface region are considerably smaller than that of the terrestrial ionosphere. At the Earth, ionospheric effects are important in the substorm process.

A highly debated question is how electrons can be accelerated to energies up to 600 keV in Mercury's magnetosphere. Eraker and Simpson discuss electron acceleration in terms of impulsive electron acceleration probably by magnetic field reconnection, and attribute the pulsations to individual particle acceleration events (Eraker and Simpson, 1986). Baker (1986) interpreted these modulations as signatures of gradient and curvature drifts of the injected energetic electrons in the hermean magnetosphere. However, a problem arising in interpreting these energetic electron fluxes as generated internally is the small hermean magnetosphere's inability to accelerate electrons to energies > 30 keV by substorm-like processes. Alternative explanations for these energetic electrons are that they are either of external origin or from the magnetospheric boundary layer (Christon, 1989). As possible external source it was suggested that jovian electrons may enter the hermean magnetosphere at the tail side during times when the planets are magnetically connected as was the case during M I (Eraker and Simpson, 1979; Baker, 1986). Based on a Tsyganenko-model specially adapted to the Mercury case, it was argued that the strong fluctuations in the magnetic field basically are the direct response of a very dynamic magnetosphere to changing solar wind parameters (Luhmann et al., 1998). The fast dynamics are a result of the low inertia of the magnetosphere because of its small size and the absence of trapped charges. In that case there is no need for energy storage and release processes, which have to be assumed for a substorm process. Also in this model, the energetic electrons would either be of external origin following open field lines or of magnetospheric boundary layer origin (Luhmann et al., 1998).

Despite the controversy about the detailed nature of the electron events the clear signature of a dipolarisation has been taken as a convincing evidence for substorm-like processes at Mercury in many publications. A final answer to this question will only be possible with more observations at Mercury to be obtained from new missions. However, even in the Earth's magnetosphere, the physical processes causing substorms are not fully understood at present.

5. Magnetosphere, exosphere, and surface coupling

The atmosphere of Mercury was found by Mariner 10 to be a surface-bound exosphere with a total pressure at the surface of $\approx 10^{-12}$ mbar that relates to gas densities at the surface of approximately 10^4 cm^{-3} for the thermal component (Broadford et al., 1976). The total column density of Mercury's exosphere considering the detected elements H, He, O, Na, and K is less than 10^{12} cm^{-2} (Hunten et al., 1988). With the ultraviolet spectrometer (UVS) on Mariner 10, the existence of neutral He (98%), atomic hydrogen (2%), and oxygen in Mercury's atmosphere has been established (Broadford et al., 1974). The oxygen abundance in the exosphere is low, comparable to that of a trace constituent of the soil. In addition, sodium (Potter and Morgan, 1985), potassium (Potter and Morgan, 1986), and calcium (Bida et al., 2000) have been detected in Mercury's exosphere via remote sensing from the Earth. The list of known and predicted constituents in Mercury's atmosphere contains the atoms H, He, O, Na, K, ^{40}Ar, ^{20}Ne, Mg, Ca, Fe, Si, S, and Al, and the molecules H_2, O_2, N_2, CO_2, H_2O, and OH according to a compilation by Killen and Ip (1999). Most certainly, this list of species is but a small portion of what is actually present. Hydrogen and helium likely originate from the solar wind and have been accreted in the crust. The other atmospheric constituents are of hermean origin.

The considered source processes to establish the atomic and molecular composition of Mercury's exosphere are diffusion (especially for the radiogenic noble gases and implanted solar wind protons), evaporation of volatiles, photon sputtering, ion sputtering, chemical sputtering, meteoritic vaporisation, and ion recombination (neutralisation) at or near the surface (Killen and Ip, 1999). Ion sputtering will result either from solar wind ions or energetic

magnetospheric ions impinging on the planetary surface. Since Mercury only has a very tenuous exosphere, charged particles injected from the magnetotail will most likely impact on the planetary surface. There are, of course, considerable uncertainties in the details of these processes arising from the largely unknown physical and chemical nature of Mercury's surface. The relative importance of the different processes will depend on latitude (ion sputtering at high latitudes, photon sputtering at low latitudes), season, dawn–dusk asymmetries, and also on the atom or molecule considered. For example, photon sputtering is important for sodium and potassium, whereas for calcium, a refractory element, ion sputtering will be the most important release mechanism. The recent observation of calcium in the vicinity of the polar regions at high exospheric temperatures provides strong support to their sputtered origin (Bida et al., 2000). For the exospheric particle distributions, the radiation pressure has also to be considered, which varies with species and also with season (Ip, 1986; Killen and Ip, 1999).

A certain fraction of these exospheric atoms and molecules will be photo-ionised. Typical photo-ionisation times are in the range between 10^4 and 10^6 s (Kumar, 1976; Killen and Ip, 1999). Thus, a fraction of these exospheric ions will become part of the magnetosphere. Possibly, these ions even dominate the ion composition for heavy elements in Mercury's magnetosphere compared to solar wind ions entering the magnetosphere directly. For example, for Na^+ ions a magnetospheric ion fraction between 10% and 50% has been estimated (Ip, 1986; Cheng et al., 1987; Othmer et al., 1999). For electrons (and protons) the observation that the plasma sheet densities at Mercury are a factor of five higher than at Earth, which is close to the ratio of solar wind densities at 0.5 and 1 AU, was taken as strong support for these electrons originating from the solar wind (Ogilvie et al., 1977).

Exospheric ions can be accelerated to considerable energies in Mercury's magnetosphere, e.g. Na^+ may have energies of keV and more according to a calculation by Cheng et al. (1987). The proposed mechanisms for acceleration are picked-up by the rapidly convecting magnetic field, sudden increase of the convection electric field, and increase in the guiding centre velocity due to slowly increasing convection electric field (Cheng et al., 1987). Moreover, initial acceleration by inductive electric fields perhaps associated with reconnection during substorm events, followed by acceleration by the cross-tail electric field during non-adiabatic interactions with the magnetic neutral sheet results in ion energies exceeding keV. Under the assumption of a tail field of 300 nT and a dipolarisation time scale of 10 s (onset of the magnetospheric substorm), it can be shown that protons and alpha particles can be accelerated up to a maximum energy of 13–14 keV, and heavy ions could be accelerated to several tens of keV (Ip, 1987). In case of a sufficiently thick and reasonably ionised exosphere, that is in case of the formation of an exoionosphere, it was argued by Lundin et al. (1997) that acceleration and heating of exospheric ions will take place in very similar ways as occurring at the topside ionosphere of the Earth. In addition to the mentioned current sheet acceleration in the magnetotail, the existence of an exoionosphere will result in an ion fountain in the cleft–cusp region due to wave-particle interaction and field-aligned acceleration associated with regions of field-aligned currents (Lundin et al., 1997).

6. Discussion and conclusions

The Mariner 10 results are incomplete in several important aspects. Firstly, the particle experiments measured primarily, if not exclusively, electrons, and moreover the measurements had a considerable gap in the covered energy range. For comparison, this is the range where most of the energy flux is observed in the terrestrial magnetosphere. Moreover, the terrestrial energy flux is contained mostly in the ions for which we do not have any information for Mercury. Thus, conclusions about acceleration processes using Mariner 10 observations, and in particular ion acceleration processes, are limited to comparisons at a phenomenological level, i.e., comparing signatures during magnetospheric substorms. Secondly, the flybys were limited in time and the complimentary information about solar wind conditions is missing. Thirdly, without adequate information about the magnetospheric plasma composition the question of magnetosphere–ionosphere coupling (or rather the surface coupling) becomes wide open to speculations and deductive arguments.

The limitations of the existing data set from Mariner 10 have to be alleviated by future missions to Mercury. For comprehensive magnetospheric observations, a future mission to Mercury should have particle instrumentation covering the energy range from about 1 eV to at least 1 MeV, both for electrons and ions. It would be desirable to measure ions even at lower energies to learn about their release processes from the surface, but spacecraft charging and its onboard control will probably not allow for that. In order to extend the observation time, an orbiting spacecraft should be foreseen, preferable in a highly elliptic orbit to visit a large fraction of the hermean magnetosphere. The simultaneous knowledge of the solar wind conditions needs a simultaneous observer outside the hermean magnetosphere. This might be achieved during phases of Mercury–Earth conjunction with near-Earth spacecraft for solar wind research, with two orbiting spacecraft at the same time (an ESA and a NASA spacecraft, see below), or with the possible realisation of the Solar Orbiter mission of ESA, which is intended to probe the solar wind close to the Sun in the range from 0.14 to 0.70 AU.

Since Mercury is so deep in the gravitational potential of the Sun, it is a difficult planet to reach and no spacecraft visited this planet since Mariner 10. Currently, there are two missions to Mercury: the Messenger mission, a NASA discovery-class mission for which the spacecraft and

Table 2
The instrument capabilities and requirements of the Mercury magnetospheric orbiter (MMO), which is one out of three elements of ESA's BepiColombo mission to planet Mercury. These instruments will share common electronics (from Balogh et al., 2000)

Instrument	Range	Mass (kg)	Average power (W)	Average TM rate (kb/s)
Magnetometer	±4096 nT	0.88	0.35	0.8
Ion spectrometer	50 eV–35 keV	4.4	4	0.5
Electron analyser	~ 1 eV–30 keV	1.1	1.2	0.1
Cold plasma detector	~ 1–50 eV	1.3	1.9	0.2
Energetic particle detector	e^-: 30–300 keV			
	p : 30 keV–6 MeV	1.2	0.7	0.04
	$Z > 1$: 7–26 MeV			
Search coil	0.1 Hz–1 MHz	1		
Electric antenna	0.1 Hz–16 MHz	2.9		
Positive ion emitter	1–100 μA	2.7	3.8	0.02
Camera	350–1000 nm	8	12	4

the instrumentation are currently being built, and the BepiColombo mission, which was recently approved as ESA cornerstone mission.

The Messenger mission is scheduled for launch in early 2004. After the Earth, Venus, and Mercury flybys the Messenger spacecraft will be inserted into an orbit around Mercury in the fall of 2009 and continue investigations for a year. The Messenger mission is mainly designed for planetary research objectives. For studies of the hermean magnetosphere, a magnetometer and an energetic particle and plasma spectrometer package will be available. The energetic particle instrument will record particles in four groups, namely protons, helium, heavy particles, and electrons. The design goal for the energy range for protons is from 20 keV up to 3 MeV. The plasma spectrometer is designed to investigate the thermal plasma in the energy range from 50 eV/e up to 15 keV/e. An electron spectrometer might be added at a later stage if resources allow. Although the energetic particle and plasma spectrometer has been primarily selected to measure the magnetospheric current system with the aim to assist separating internal from external magnetic fields when deconvolving the magnetometer data, it will also provide the first measurements of the ion component in Mercury's magnetosphere.

For the BepiColombo mission three modules are foreseen, a planetary orbiter, a magnetospheric orbiter, and a landing module. The three modules will be travelling to Mercury either together as a single spacecraft or will be spilt up into two spacecrafts possibly with a large time gap in between (Balogh et al., 2000). Each module is optimised for its scientific objective. The nominal mission concept foresees arrival at Mercury and insertion into a stable orbit late 2012 with a mission duration of at least one year. The magnetospheric orbiter, the module that is of concern for the topic of this review, might be advanced to reach Mercury already in early 2010. The magnetospheric orbiter will have a full and state-of-the-art complement of instruments for magnetospheric research that are listed in Table 2.

The smaller size of the hermean magnetosphere and the higher solar wind pressure result in a much more dynamic magnetosphere than at Earth, probably the most dynamic in the solar system. The time when the hermean magnetosphere needs to adjust to new solar wind conditions is comparable with the solar wind transient time, which has been estimated to be around 1 min (Luhmann et al., 1998). Furthermore, the relevant parameter for the substorm process is the convection time, which is also around 1 min and which is the shortest of all planets (Ip, 1997). Thus, the time resolution of the particle and fields instrumentation should be even better. In addition, it might be advantageous to complement the proposed classic suite of particle instruments for in situ magnetospheric plasma research with a neutral particle imaging instrumentation for remote sensing, as was suggested already earlier (Lundin et al., 1997). This new technique records the two-dimensional instantaneous distributions of plasma particles with high temporal resolution (Wurz, 2000). Remote sensing via neutral particle imaging is currently employed on the IMAGE mission of NASA to visualise the Earth's magnetosphere and is foreseen for the Mars Express mission of ESA to investigate Mars' environment.

The discovery of the atomic sodium exosphere at Mercury has important implications for the planetary magnetosphere and surface. The high-latitude enhancements were seen as an evidence of magnetospheric processes, or local surface concentration enhancements. Since there is also a time dependent variation on time scales of less than a day (Potter et al., 1999), at least some of the Na and K enhancements must be of non-geologic origin. The processes releasing atoms and molecules from Mercury's surface will not promote different species into the exosphere (and subsequently into the magnetosphere) in proportion to their surface abundances. For example, it has been argued that protons and sodium ions have comparable densities and oxygen ions will only be a minor constituent in the magnetosphere (Cheng et al., 1987). Thus, it would be highly desirable to carry instruments capable of investigating Mercury's tenuous atmosphere. However, it is generally accepted that the composition of the exosphere and possibly the magnetosphere is related to that

of the regolith and crust. Thus, from measurements of the composition of the exosphere and magnetosphere it will also be possible to deduce some information about the elemental and chemical composition of the regolith and the crust.

Acknowledgements

The authors thank J. Weygand of the University of Bern for carefully reading the manuscript. This work was supported by the Swiss National Science Foundation.

References

Armstrong, T.P., Krimigis, S.M., Lanzerotti, L.J., 1975. A reinterpretation of the reported energetic particle fluxes in the vicinity of Mercury. J. Geophys. Res. 80 (28), 4015–4017.

Armstrong, T.P., Lanzerotti, L.J., Krimigis, S.M., 1979. Comment on Electron calibration of instrumentation for low energy, high intensity particle measurements at Mercury by Christon, Daly, Eraker, Perkins, Simpson, and Tuzzolino. J. Geophys. Res. 84 (A8), 4468–4471.

Baker, D.N., 1986. Jovian electron populations in the magnetosphere of Mercury. Geophys. Res. Lett. 13 (8), 789–792.

Baker, D.N., Simpson, J.A., Eraker, J.H., 1986. A model of impulsive acceleration and transport of energetic particles in Mercury's magnetosphere. J. Geophys. Res. 91 (A8), 8742–8748.

Balogh, A., Bird, M., Blomberg, L., Bochsler, P., Bougeret, J.-L., Brückner, J., Iess, L., Guest, J., Langevin, Y., Milani, A., Sauvaud, J.-A., Schmidt, W., Spohn, T., von Steiger, R., Thomas, N., Torkar, K., Wänke, H., Wurz, P., 2000. BepiColombo—an interdisciplinary cornerstone mission to the planet Mercury, Noordwijk. The Netherlands, European Space Agency, ESA-SCI(2000)1.

Bida, T.A., Killen, R.M., Morgan, T.H., 2000. Discovery of calcium in Mercury's atmosphere. Nature 404, 159–161.

Broadford, A.L., Kumar, S., Belton, M.J.S., McElroy, M.B., 1974. Mercury's atmosphere from Mariner 10: preliminary results. Science 185, 166–169.

Broadford, A.L., Shemansky, D.E., Kumar, S., 1976. Mariner 10: Mercury atmosphere. Geophys. Res. Lett. 3 (10), 577–580.

Cheng, A.F., Johnson, R.E., Krimigis, S.M., Lanzerotti, L.J., 1987. Magnetosphere, exosphere, and surface of Mercury. Icarus 71, 430–440.

Christon, S.P., 1987. A comparison of the Mercury and Earth magnetospheres: electron measurements and substorm time scales. Icarus 71, 448–471.

Christon, S.P., 1989. Plasma and energetic electron flux variations in the Mercury 1 C event: evidence for a magnetospheric boundary layer. J. Geophys. Res. 94 (A6), 6481–6505.

Christon, S.P., Daly, S.F., Eraker, J.H., Perkins, M.A., Simpson, J.A., Tuzzolino, A.J., 1979. Electron calibration of instrumentation for low energy, high intensity particle measurements at Mercury. J. Geophys. Res. 84 (A8), 4277–4288.

Connerney, J.E.P., Ness, N.F., 1988. Mercury's magnetic field and interior. In: Vilas, F., Chapman, C.R., Matthews, M.S. (Eds.), Mercury. The University of Arizona Press, Tucson, pp. 514–561.

Eraker, J.H., Simpson, J.A., 1979. Jovian electron propagation close to the Sun ($\leqslant 0.5$AU). Astrophys. J. 232, L131–L134.

Eraker, J.H., Simpson, J.A., 1986. Acceleration of charged particles in Mercury's magnetosphere. J. Geophys. Res. 91 (A9), 9973–9993.

Goldstein, B.E., Suess, S.T., Walker, R.J., 1981. Mercury: magnetospheric processes and the atmospheric supply and loss rates. J. Geophys. Res. 86 (A7), 5485–5499.

Grard, R., 1997. Photoemission of the surface of Mercury and related electrical phenomena. Planet. Space Sci. 45 (1), 67–72.

Grard, R., Laakso, H., Pulkkinen, T.I., 1999. The role of photoemission in the coupling of the Mercury surface and magnetosphere. Planet. Space Sci. 47, 1459–1463.

Hunten, D.M., Morgan, T.H., Shemansky, D.E., 1988. The Mercury atmosphere. In: Vilas, F., Chapman, C.R., Matthews, M.S. (Eds.), Mercury. The University of Arizona Press, Tucson, pp. 562–612.

Ip, W.-H., 1986. The sodium exosphere and magnetosphere of Mercury. Geophys. Res. Lett. 13 (5), 423–426.

Ip, W.-H., 1987. Dynamics of electrons and heavy ions in Mercury's magnetosphere. Icarus 71, 441–447.

Ip, W.-H., 1997. Time-variable phenomena in the magnetosphere and exosphere of Mercury. Adv. Space Res. 19 (10), 1615–1620.

Kabin, K., Gombosi, T.I., DeZeeuw, D.L., Powell, K.G., 2000. Interaction of Mercury with the solar wind. Icarus 143, 397–406.

Killen, R.M., Ip, W.H., 1999. The surface-bounded atmosphere of mercury and the moon. Rev. Geophys. 37 (3), 361–406.

Kumar, S., 1976. Mercury's atmosphere: a perspective after Mariner 10. Icarus 28, 579–591.

Luhmann, J.G., Russell, C.T., Tsyganenko, N.A., 1998. Disturbances in Mercury's magnetosphere: are the Mariner 10 "substorms" simply driven? J. Geophys. Res. 103 (A5), 9113–9119.

Lundin, R., Barabash, S., Brandt, P., Eliasson, L., Nairm, C.M.C., Norberg, O., Sandahl, I., 1997. Ion acceleration processes in the hermean and terrestrial magnetospheres. Adv. Space Res. 19 (10), 1593–1607.

McPherron, R.L., Russell, C.T., Aubry, M.P., 1973. Satellite studies of magnetospheric substorms on August 15, 1968. J. Geophys. Res. 78 (16), 3131–3148.

Ness, N.F., 1979. The magnetosphere of Mercury. In: Kennel, C.F., Lanzerotti, L.J., Parker, E.N. (Eds.), Solar System Plasma Physics, Vol. II. North Holland, Amsterdam, pp. 183–206.

Ness, N.F., Behannon, K.W., Lepping, R.P., Whang, Y.C., Schatten, K.H., 1974a. Magnetic field observations near Venus: preliminary results from Mariner 10. Science 183, 1301–1306.

Ness, N.F., Behannon, K.W., Lepping, R.P., Whang, Y.C., Schatten, K.H., 1974b. Magnetic field observations near Mercury: preliminary results from Mariner 10. Science 185, 151–160.

Ness, N.F., Behannon, K.W., Lepping, R.P., Whang, Y.C., 1975a. Magnetic field of Mercury confirmed. Nature 255, 204–205.

Ness, N.F., Behannon, K.W., Lepping, R.P., Whang, Y.C., 1975b. The magnetic field of Mercury. 1. J. Geophys. Res. 80 (19), 2708–2716.

Ness, N.F., Behannon, K.W., Lepping, R.P., Whang, Y.C., 1976. Observations of Mercury's magnetic field. Icarus 28, 479–488.

Ogilvie, K.W., Scudder, J.D., Hartle, R.E., Siscoe, G.L., Bridge, H.S., Lazarus, A.J., Asbridge, J.R., Bame, S.J., Yeates, C.M., 1974. Observations at Mercury encounter by the plasma science experiment on Mariner 10. Science 185, 145–151.

Ogilvie, K.W., Scudder, J.D., Vasyliunas, V.M., Hartle, R.E., Siscoe, G.L., 1977. Observations at the planet Mercury by the plasma electron experiment: Mariner 10. J. Geophys. Res. 82 (13), 1807–1824.

Othmer, C., Glassmeier, K.-H., Cramm, R., 1999. Concerning field line resonances in Mercury's magnetosphere. J. Geophys. Res. 104, 10369–10378.

Potter, A.E., Morgan, T.H., 1985. Discovery of sodium in the atmosphere of Mercury. Science 229, 651–653.

Potter, A.E., Morgan, T.H., 1986. Potassium in the atmosphere of Mercury. Icarus 67, 336–340.

Potter, A.E., Killen, R.M., Morgan, T.H., 1999. Rapid changes in the sodium exosphere of Mercury. Planet. Space Sci. 47, 1441–1448.

Russell, C.T., 1989. ULF waves in the Mercury magnetosphere. Geophys. Res. Lett. 16 (11), 1253–1256.

Russell, C.T., Baker, D.N., Slavin, J.A., 1988. The magnetosphere of Mercury. In: Vilas, F., Chapman, C.R., Matthews, M.S. (Eds.), Mercury. The University of Arizona Press, Tucson, pp. 514–561.

Simpson, J.A., Eraker, J.H., Lamport, J.E., Walpole, P.H., 1974a. Search by Mariner 10 for electrons and protons accelerated in association with Venus. Science 183, 1318–1321.

Simpson, J.A., Eraker, J.H., Lamport, J.E., Walpole, P.H., 1974b. Electrons and protons accelerated in Mercury's magnetic field. Science 185, 160–166.

Siscoe, G.L., Ness, N.F., Yeates, C.M., 1975. Substorms on Mercury? J. Geophys. Res. 80 (31), 4359–4363.

Slavin, J.A., Owen, J.C.J., Connerney, J.E.P., Christon, S.P., 1997. Mariner 10 observations of field-aligned currents at Mercury. Planet. Space Sci. 45 (1), 133–141.

Whang, Y.C., 1977. Magnetospheric magnetic field of Mercury. J. Geophys. Res. 82 (7), 1024–1030.

Whang, Y.C., 1979. Model magnetosphere of Mercury. Phys. Earth Planet. Inter. 20, 218–230.

Wurz, P., 2000. Detection of energetic neutral atoms. In: Scherer, K., Fichtner, H., Marsch, E. (Eds.), The Outer Heliosphere: Beyond the Planets. Copernicus Gesellschaft e.V, Katlenburg-Lindau, Germany, pp. 251–288.